

Development and investigation of a non-catalytic self-aspirating meso-scale premixed burner integrated thermoelectric power generator



Tanuj Singh*, Richard Marsh, Gao Min

Cardiff School of Engineering, Cardiff University, Cardiff CF24 3AA, Wales, UK

ARTICLE INFO

Article history:

Received 6 November 2015

Accepted 8 March 2016

Keywords:

Thermoelectric power generation

Seebeck effect

Premixed combustion

Meso-scale

Non-catalytic

ABSTRACT

Portable electrical power generation using hydrocarbons presents significant potential owing to their higher power densities and negative environmental factors associated with chemical cell batteries. Small scale combustors have been widely developed and tested for power generation purposes, employing thermoelectrics and thermo-photovoltaic conversion of combustion heat into electricity. This experimental study is concerned with development and investigation of a novel non-catalytic meso-scale self-aspirating premixed burner with integrated thermoelectric generator which can be used in remote places to generate electricity for a continuous period of one month. Flame stabilisation has been one of the main issues in small scale combustion systems due to higher surface to volume ratio associated with small size of the combustor. Previous research has shown that catalytic combustion is one way of improving flame stabilisation, however employing a catalyst into the system increases the manufacturing cost which can be a significant downside. This research work studies flame stabilisation mechanisms in meso-scale burner which mainly focuses on backward facing step and secondary air addition into the combustion chamber. The first phase of the research was involved development of the burner which included optimisation of the design to achieve a stable enclosed premixed flame as per the design and operational requirements. The second phase of the research focused on the integration of the burner with thermoelectric power generators. This involved investigation of various configurations to optimise the electrical power output when limited amount of heat is available. The relationship between ambient temperature and thermoelectric power generation using an environmentally controlled chamber has also been presented in this experimental study.

© 2016 The Authors. Published by Elsevier Ltd. This is an open access article under the CC BY license (<http://creativecommons.org/licenses/by/4.0/>).

1. Introduction

Thermoelectric power generation using small scale combustion of hydrocarbons is a promising alternative to conventional means of generating electricity. It is reported that hydrocarbons have notably higher energy density when compared to chemical cell batteries. For example, propane has a specific energy of 40 MJ kg^{-1} whereas a lithium-ion battery has 0.5 MJ kg^{-1} [1]. Batteries require long recharging durations and there are several environmental issues associated with their disposal. It is estimated that less than 3% of lithium-ion batteries are recycled, the rest being landfilled [2]. There are several benefits of thermoelectric power generation such as high reliability, noiseless operation, inexpensive maintenance and long life [3,4]. This research work involves a detailed study of integration of thermoelectric power generation modules

with small combustors. The principle of thermoelectric power generation is based on Seebeck effect which states that a voltage is generated when there is a temperature difference at the two junctions of semiconductors joined together [5]. Modern thermoelectric generator (TEG) modules are fabricated using n-type and p-type semiconductors connected electrically in series. In the thermoelectric-burner integrated systems, combustion of hydrocarbons such as propane provides the heat required to raise the temperature of the hot side of a TEG module while cooling is provided at the cold side via heat exchangers or cold water recirculation.

A small scale thermoelectric power generation device employing combustion is presented in this work. The application of this device is in remote areas where mains electricity is not easily available. An application can be found in pest control industry where insect traps can be powered in gardens or farms by such unit while subsequently using the combustion exhaust (carbon dioxide and water) to attract insects [6]. Other applications can be in military and in parts of developing countries where electricity is not

* Corresponding author.

E-mail addresses: sbstds@cardiff.ac.uk (T. Singh), MarshR@cardiff.ac.uk (R. Marsh), Min@cardiff.ac.uk (G. Min).

Nomenclature

Symbol	Definition		
P	power output, Watt (W)	T_{H1}	average hot side temperature in primary power generator, Kelvin (K)
P_1	power output of primary power generator, Watt (W)	T_{H2}	average hot side temperature in secondary power generator, Kelvin (K)
P_2	power output of secondary power generator, Watt (W)	T_C	average cold side temperature of TEGs, Kelvin (K)
P_{max}	maximum power, Watts (W)	T_{C1}	average cold side temperature in primary power generator, Kelvin (K)
R_i	internal resistance of TEG, Ohms (Ω)	T_{C2}	average cold side temperature in secondary power generator, Kelvin (K)
V_L	matched load voltage, Volts (V)	V_f	fuel flow rate, Litres per minute ($L \text{ min}^{-1}$)
V_{L1}	matched load voltage of primary power generator, Volts (V)	Abbreviations	
V_{L2}	matched load voltage of secondary power generator, Volts (V)	TEG	thermoelectric generator
ΔT	average temperature difference across the TEGs, Kelvin (K)	HE	heat exchanger
ΔT_1	average temperature difference in primary power generator, Kelvin (K)	IHS	internal heat sink
ΔT_2	average temperature difference in secondary power generator, Kelvin (K)		
T_H	average hot side temperature of TEGs, Kelvin (K)		

available. The device was developed with a focus on low cost and realistic stand-alone design having potential for commercialisation. The device was designed to operate continuously for a month when connected to a 13 kg propane gas bottle, which means that it can provide small electrical power without any disruption for 30 days and the user would only have to change the gas bottle once in a month. The emphasis was given to eliminate the requirement of moving parts such as pumps and combustion air compressors because of the electricity required to operate them and to reduce the manufacturing cost, therefore, making it a practical design solution.

Various small scale power generators, employing thermoelectrics and combustion, have been reported in the past. Yadav et al. [7] performed experimental investigation on a micro power generator consisting of thermoelectric power generation (TEG) modules integrated with a micro-combustor (thermal input ~ 5 W). Their non-catalytic micro-burner were designed to preheat inlet reactants and employed multiple backward facing steps for flame stabilisation. The maximum power generation using two and four modules is reported to be 1.56 W and 2.35 W respectively. Nortan et al. [8] developed and tested a micro catalytic burner for power generation using thermoelectrics having a thermal output of 150 W and 0.5 W electrical power generation. A catalytic combustion based thermoelectric power generator is reported by Xiao et al. [9], the thermal output of the burner was around 500 W and generated ~ 8 W of electrical power using eight thermoelectric modules. A catalytic propane burner is developed by Merotto et al. [10] for integration with commercially available thermoelectric modules. The combustion efficiency is reported to be 96% and the electrical power generation 9.86 W using two TEG modules [11]. Mustafa et al. [12] developed and investigated a hexagonal shaped porous gas (butane) burner, thermal output of ~ 1.6 kW, for power generation using six thermoelectric modules. The maximum power output reported is 1.05 W. In another research, Mustafa et al. [13] used liquid fuel, kerosene-vegetable cooking oil, in a porous catalytic burner which had 10 TEG modules attached to it. The power generation was in a range of 4–21.9 W, depending upon the operating parameters. Mueller et al. [14] conducted a research on employing super-adiabatic porous catalytic burner in thermoelectric generators. The maximum power was recorded to be around 0.3 W after 5 h of operation using one TEG. An example of integration of thermoelectric to a comparatively larger scale of combustion (thermal output of up to

150 kW) can be seen in the work of Aranguren et al. [15] where they attached 48 TEG modules to the chimney of a combustion chamber. The electrical power generated is reported to be 21.56 W. In order to achieve high power densities, new thermoelectric modules were developed by Zhang et al. which consisted of nanostructured bulk half-Heusler alloys [16]. They have reported a power output of 94.5 W using 8 TEG modules integrated into a residential boiler. A thermoelectric generator hybrid system consisting of direct-carbon-fuel-cell is reported by Zhao et al. [17]. Hasani and Rahbar [18] reported a waste heat recovery system using thermoelectrics from a ~ 5 kW PEM (proton exchange membrane) fuel cell, employing four TEG modules, they were able to produce 0.5 W of electrical power at a temperature difference of 20 K.

Some recent experimental work carried out in recovering waste heat from combustion appliances, such as stoves, using TEG modules can be found in the study of Montecucco et al. [19] and O'Shaughnessy et al. [20]. The former reported 27 W electrical power output using four TEG modules at a temperature difference of 250 K; and the later around 5 W using one TEG.

The scale of the burner presented in this study has been classified based on the previous work done by various authors in small scale combustion. Kariuki and Balachandran [21] developed a burner having combustion chamber made up of 5 channels, it was operated at a thermal output of 25–250 W and has been classified as a micro-combustor. Nortan et al. [8] developed and tested a catalytic burner having a thermal output of 150 W and termed it as micro-burner. Similar examples of combustors classified under micro-scale are the burners developed by Kania and Dreizler [22] (burner rating 50 W), US government [23] and Li et al. [26]. In the work of Wu et al. [24], a clear differentiation among micro and meso-scales has not been shown and their thermal outputs are between 25 and 170 W. Therefore, based on the operating range or burner thermal output, the burner developed and tested in the present study can be classified as micro-scale combustor as their thermal output is ≤ 250 W, which is similar to the above discussed micro-combustors. However, a comparison based on the dimensions showed that the combustion chamber in present study was significantly bigger than those developed by the other investigators. The micro burner developed by US government had a characteristic length of just 1 mm, also the combustion chamber in Kania and Dreizler's burner was 25 mm long and the diameter was just 4 mm and the micro combustors of Kariuki and

Balachandran had combustion chamber 3 mm wide, 27 mm long and 1 mm high. It is evident that the size of all these combustion chambers of micro scale burners is substantially smaller than the combustion chamber of the present work which has a diameter of 20 mm and length 30 mm. This suggests that classifying the burners of this study as micro may not be justified based on their large combustion chamber size. It is worth noticing here that Belmont et al. developed burner which was operated at a thermal power output of 75 W and they have classified it as a meso-scale burner [25]. So considering the comparatively large dimensions of the burner and micro-scale operating parameters, the burner of the present study is classified as meso-scale.

It is also pertinent to note that the combustion based thermoelectric power generation devices operating at sub-kilowatt thermal output range, as reported in the literature above, employ catalyst in their burners, whereas the device presented in this paper consists of a non-catalytic burner. Another novel aspect of the present combustion-based thermoelectric generator is self-aspiration of combustion air, which makes the device practicable as the need of additional power to run auxiliary components such as compressor pump is eliminated.

The first phase of the research was concerned with development of the burner which included design optimisation to achieve a stable enclosed premixed flame as per the operational requirements. The second phase of the research focused on the integration of the burner with thermoelectric power generators. This involved investigation of various configurations, designed on the basis of varying the number of thermoelectric modules and their placement on the burner, to optimise the electrical power output.

2. The meso-scale burner

The motivation behind the design of the burner was a premixed gas burner which offers a good mixing mechanism for the reactants, a flame stabilisation mechanism which facilitates combustion at the desired location, and can accommodate TEG modules on its sides. Premixed combustion is characterised as a flame where the reactants (fuel and air) are mixed before entering the

flame zone, whereas in a diffusion-type flame, the mixing and combustion take place simultaneously.

The burner was designed to operate at a constant thermal output of 250 W, which corresponds to 150 mL min^{-1} of propane injection (based on the higher heating value of propane). A 13 kg gas bottle will last 30 days at 150 mL min^{-1} of fuel supply to the burner, thus fulfilling the operating requirement as mentioned previously. A photograph of the burner is shown in Fig. 1(a); it was machined from a single 130 mm long, 40 mm square cross-section 316 Stainless Steel bar. The square shape was chosen to accommodate TEG modules on its external sides. Another feature of this burner was self-aspiration of combustion air, for this purpose, two holes having diameter 7 mm were machined on all the sides of the burner to vary the air supply as shown in Fig. 1(a) and (b). The burner was provided with a premixing zone, as shown in Fig. 1(b), which is a smaller diameter passage that mixes the air as it enters into the combustion chamber. A backward facing step was employed in the design to enhance mixing of reactants due to formation of recirculation zones in the flow [27–29]. To address the issue of flame stabilisation and combustion efficiency, secondary air was added into the combustion chamber. Secondary air was found to provide aerodynamic stability and ensure that enough air was available for complete combustion of the fuel. Focus was given to utilising or capturing the optimum amount of heat from the exhaust gas to convert it into electricity using TEG modules. The electrical power generation by a TEG module is directly proportional to the temperature difference across its two sides. The more heat available at the module's hot side, the higher will be the temperature difference and hence, greater electrical power output can be achieved. Thus, the idea was to keep the external shape of the burner square and its width the same as the width of a standard TEG module, which would ensure that the module covers the maximum surface area of the burner's side and hence less heat losses.

Propane was used as fuel which was supplied from a 13 kg bottle through a low pressure (37 mbar) gas regulator. The fuel was regulated using a NGX PLATON GTF flowmeter ranged $40\text{--}300 \text{ mL min}^{-1}$ calibrated for propane.

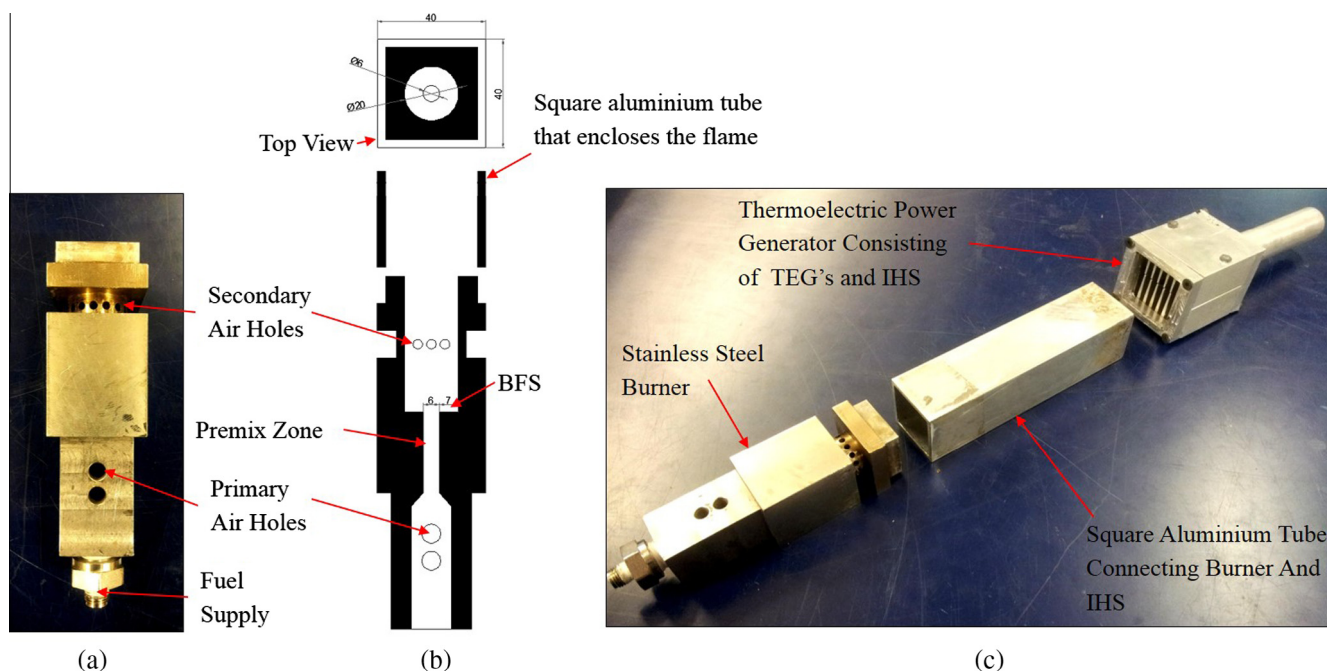


Fig. 1. (a) Photograph of meso-scale stainless steel burner, (b) a 2-D schematic of the burner showing the main features and important dimensions, and (c) photograph showing the main components of the thermoelectric and combustion integrated electrical power generator.

During operation, propane is supplied through the rotameter flow meter to the brass jet nozzle which injects it into the primary mixing zone where it entrains air from the ambient through primary air holes due to creation of a low pressure zone inside. The reactants move downstream into the premix zone and finally into the combustion chamber which consists of the backward facing step. As shown in Fig. 1, holes for secondary air entrainment are machined above the backward facing step. The method of secondary air supply is same as primary air i.e. the air is entrained into the combustion chamber by the downstream fuel and air mixture.

It should be noted here that these experiments were carried out without any forced air supply i.e. the burners were operating under self-aspiration mode. At constant fuel flow rate the only way to vary the air supply was to change the effective area of the air holes provided in the primary mixing zone. Therefore, it was not possible to directly measure the air to fuel ratio, and hence equivalence ratio, so this was estimated based on data from the gas analysis system (shown later). The effective area available for primary air entrainment was 38.5 mm², 77 mm², 115 mm² and 154 mm² for 1, 2, 3 and 4 holes respectively.

During stable operation it was observed that the flame was anchored on the secondary air holes, and this allowed for a broad operating envelope (between stable rich and lean operation) at a variety of fuel flow rates as shown later.

Fig. 2 shows photographs of the flame obtained at fuel flow rates (V_f) ranging from 100 mL min⁻¹ to 200 mL min⁻¹ with two primary air holes open. As previously stated, the burner was designed to operate at 150 mL min⁻¹ of propane injection into the combustion chamber and at this flow rate it produced a visibly clean burning, stable premixed flame anchored at the secondary air holes. The flame was less stable at lower flow rates of propane as shown in Fig. 2(c) and (d) and at 200 mL min⁻¹ of propane flow rate the flame attained a yellow tip (Fig. 2(b)).

Exhaust gas analysis was carried out using an integrated system developed by Signal Instruments comprising of several analysers. It employed a Flame Ionisation Detector (FID) within a Signal 3000 HM to detect total Hydrocarbons (THCs), calibrated with propane in the range 0–890 ppm. It simultaneously employed a heated vacuum chemiluminescence analyser (Signal 4000 VM) to quantify NO_x concentrations calibrated to 37.1 ppm NO and 1.9 ppm NO₂. The system also contained a multi-gas analyser (Signal MGA), consisting of an infrared cell for measurement of CO (calibrated for 0–900 ppm) and CO₂ 0–9%, in addition to a paramagnetic O₂ sensor (up to 22.5%).

The total exhaust was determined using stoichiometric equation of propane and conservation of mass through the burner. The average percentage of CO₂ in the exhaust shown by the multi-gas analyser was 5.2% while average O₂ was 12.93%. The burner was set up at 150 mL min⁻¹ of propane, which should produce 450 mL min⁻¹ of CO₂ at stoichiometric conditions. Using the stoichiometric equation for propane, the total exhaust is calculated to be ~9 L min⁻¹ (at adiabatic flame temperature of propane) as the burner is producing 0.450 L min⁻¹ of CO₂ at stoichiometry which was 5.2% of total exhaust shown by the gas analyser. The

concentration of CO was 72.5 ppm which corresponds to 0.65 mL min⁻¹ by volume and average NO_x was 29 ppm corresponding to 0.25 mL min⁻¹ by volume. There were no measurable traces of un-burnt hydrocarbons in the exhaust indicating complete combustion of propane. The absence of un-burnt hydrocarbons and low concentration of compounds such as CO and NO_x shows that the addition of secondary air not just only helped in achieving a stable combustion but also contributed towards clean and efficient combustion.

3. Integration with thermoelectrics

The meso-scale premixed burner described in the previous section was integrated with TEG modules. The design consideration in thermoelectric optimisation was to achieve higher electrical power with the minimum number of modules used through an efficient means of heat dissipation at the cold side and heat absorption from the combustion exhaust at the hot side to maximise temperature difference under steady-state conditions. Higher temperature difference is desired as electrical power output is directly proportional to the temperature difference across the two sides of the TEG module [30–34]. In this section, results from optimisation of the hot side of the TEG module are presented which includes identifying a mechanism to increase the hot side temperature of the module to achieve a higher temperature difference. Subsequently design configurations were tested, which consisted of varying the arrangement of TEG modules and heat exchangers.

The TEG modules used in the experiments were obtained from European Thermodynamics Limited, UK. The dimensions of the module are 40 ± 0.5 mm × 40 ± 0.5 mm × 3.4 ± 0.1 mm, consisting of 254 bismuth-telluride thermo-elements. Laboratory characterisation was carried out to determine the internal resistance of the module which is required when measuring the maximum power generated by the thermoelectric burner assembly. The characterisation involved measuring electrical power output at various values of load resistance while maintaining a constant temperature difference across the TEG by varying the heat input and removal at hot and cold sides respectively. The electrical power generation is maximum when at the internal resistance of the TEG i.e. the matched load condition [35]. The electrical power was found to be highest at 2.6 Ω, therefore in the experiments performed in this study for the measurement of electrical power, a 2.6 Ω resistor was connected in series with the TEG module as load on the system to calculate P_{max} . As mentioned earlier, various different configurations have been tested in the present research which consisted of using a combination of one or more TEG modules. They were connected in series when more than one module was used. An ISO-TECH 70 Series Compact Multimeter CAT IV IDM73 was used which has a DC voltage accuracy of ±0.5%, DC current accuracy ±1%, and resistance accuracy ±0.7%.

To measure the hot side temperature (T_H), a k-type thermocouple, having a 0.20 mm probe diameter, was placed inside a groove on the burner wall where the TEG module was placed while

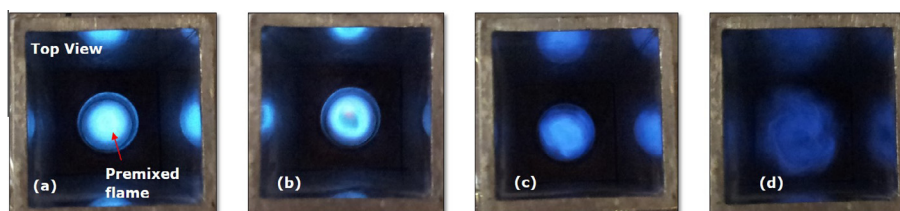


Fig. 2. Photographs of the flame (a) $V_f = 150$ mL min⁻¹, 2 air hole, (b) $V_f = 200$ mL min⁻¹, 2 air holes, (c) $V_f = 125$ mL min⁻¹, 2 air holes, and (d) $V_f = 100$ mL min⁻¹, 2 air holes.

making sure the module and burner wall were in thermal contact with each other. To measure the cold side temperature (T_C), a k-type thermocouple was placed between the TEG module and cold side heat exchanger while maintaining thermal contact between them. The temperature measurements were recorded using a handheld digital thermocouple reader, with an accuracy of $\pm 0.2\%$. The hot (T_H) and cold (T_C) side temperatures shown in the results are the average hot and cold side temperature of the TEG's in a power generator. Silicon thermal paste was used in the experiments to maintain a good thermal contact between TEG and burner wall on the hot side of the module and TEG and heat exchanger on the cold side of the module. The composition of the paste is 60–80% Aluminium Oxide and 10–30% Zinc Oxide. The thermal conductivity of the paste is $2.9 \text{ W m}^{-1} \text{ K}^{-1}$.

3.1. Hot side optimisation

One way to optimise temperature difference is by maximising the hot side temperature (T_H). Fig. 1(c) shows the stainless steel burner consisting of the fuel nozzle, mixing zones and combustion chamber; and the square aluminium tube on which the TEGs were placed in this particular experiment. The hot side of the TEG was in contact with the burner wall while the cold side was provided with a heat exchanger. As previously stated, all tests were undertaken at a fixed burner thermal output. Hence, a design feature was sought which would help in achieving a high T_H by extracting the limited heat available from the burner. The placement/location of the TEG module on the burner is important as it determines how much heat is flowing through it. The results showed that the T_H without TEG modules was around 573 K and the T_H after placing TEG modules on the burner wall was around 438 K, attributed to heat conduction through the TEG modules. There was a significant drop in the wall temperature when modules were placed on it, as shown in Fig. 3.

In order to increase the temperature of the hot side of the module, an aluminium internal heat sink (IHS) with internal fins was connected to the burner tube with the aim of extracting more heat from exhaust gases as shown in Fig. 1(c). The internal fins were provided to increase the surface area in contact with the exhaust gases which will result in increased heat transfer to the module and hence, higher T_H . The TEG modules were placed on the two opposite sides of the IHS. Fig. 3 shows a comparison of temperature

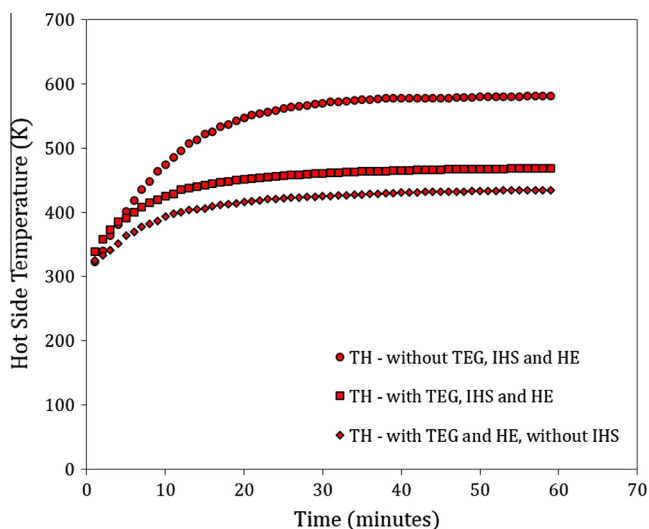


Fig. 3. Graph showing hot side temperature for three design configurations: (i) without TEG, HE, and IHS; (b) with TEG and HE but without IHS; and (iii) with TEG, HE and IHS in the unit.

profiles obtained with the three design configurations tested. The results showed an increase in the T_H from 438 K without IHS to 470 K with IHS.

3.2. Design optimisation

Three configurations were tested with the objective of optimising power generation. These configurations differ from each other on the basis of number of heat exchangers and their orientation, number of internal heat sinks and number of TEG modules employed; and thus a comparison between these configuration options was essential.

Firstly, 'nominal configuration' will be described, the schematic diagram of which is shown in Fig. 4(a) and a photograph of tests being carried out on the nominal configuration is shown in Fig. 4 (b). This was constructed and assembled based on the results from the hot side optimisation design stage. This design configuration consisted of two TEG modules placed on the opposite sides of internal heat sink. The cold side heat exchangers were two 500 mm long, 40 mm wide extruded aluminium profiles and the height of the fins was 70 mm. Experiments were performed on various modified versions of the nominal configuration and a comparison of results was carried out, shown later.

The matched load voltage and current are shown in Fig. 5(a) and (b) shows matched load power output as a function of temperature difference. It can be seen that the matched load voltage increased from 1.46 to 4.25 V; and the matched load current increased from 0.26 to 0.83 A with increase in temperature difference from 25 to 88 K. The increase in current and voltage is reflected in the power output, which increased from 0.36 to 3.54 W. This upward trend can be explained by the Seebeck principle, which is given as $V_S = n\alpha\Delta T$, where V_S is the Seebeck voltage, n is the number of thermoelements in the TEG, α is the Seebeck Coefficient and ΔT is the temperature difference across the TEG. It is obvious that higher temperature difference will generate higher Seebeck voltage, and hence higher will be the power output. At 250 W heat input, the electrical power generation was around 3.54 W corresponding to 4.25 V of load voltage at a temperature difference of 88 K. These results were considered as a basis of comparison with the results from three modified versions of nominal configuration. The thermal contact between the TEG and the hot and cold sides can have a significant effect on the power output. Also, the compression force on the module can influence the electrical performance of the TEG. As the assembly is done manually, the error associated with the thermal contact and compression force on the module was around 5%.

It should be noted that the term 'power generator' will be used from hereafter which refers to an assembly of internal heat sink and thermoelectric module(s). A schematic example of a power generator can be seen in Fig. 6(a) consisting of two TEG modules placed on the opposite sides of the IHS. The hot side of the module is in thermal contact with IHS and the cold side is in thermal contact with the heat exchanger for heat dissipation.

3.2.1. Configuration 1

Fig. 6(a) shows schematic of configuration 1 which consisted of two power generators connected downstream of the burner tube, as compared to one in the nominal configuration. The number of TEG modules in each power generator was two, therefore this configuration employed four modules in total. As shown in Fig. 6, each cold side heat exchanger was shared by two modules.

The concept behind this design change was to recover the available remaining heat from the exhaust after it has passed through the first internal heat sink, and using two additional TEG modules to convert this recovered heat into electricity. Fig. 6(b) shows a photograph of configuration 1, the following results were obtained

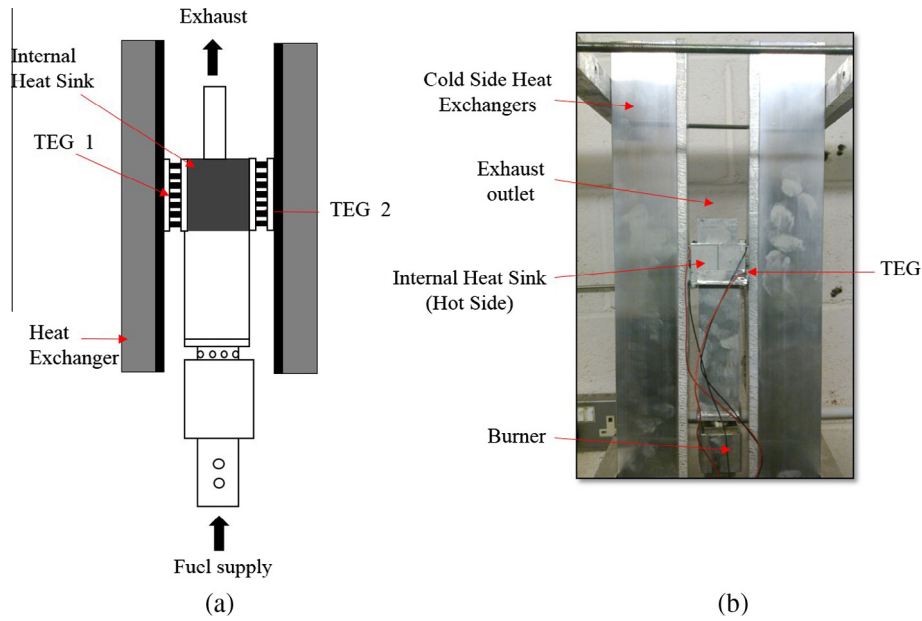


Fig. 4. (a) Schematic diagram, and (b) a photograph of 'nominal configuration' showing the main components.

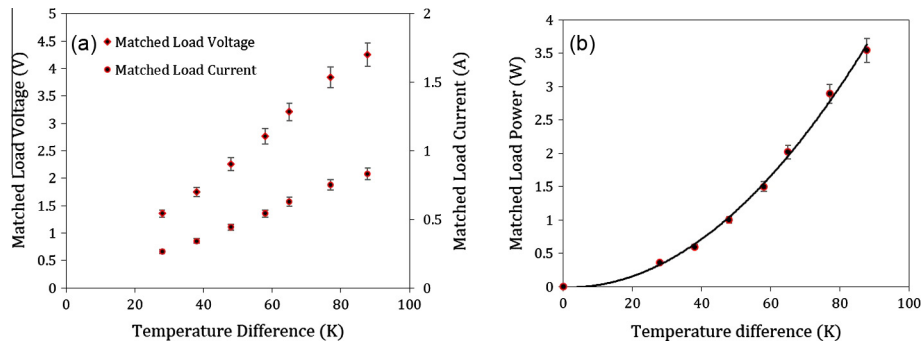


Fig. 5. (a) Matched load voltage and current, and (b) matched load power output as a function of temperature difference.

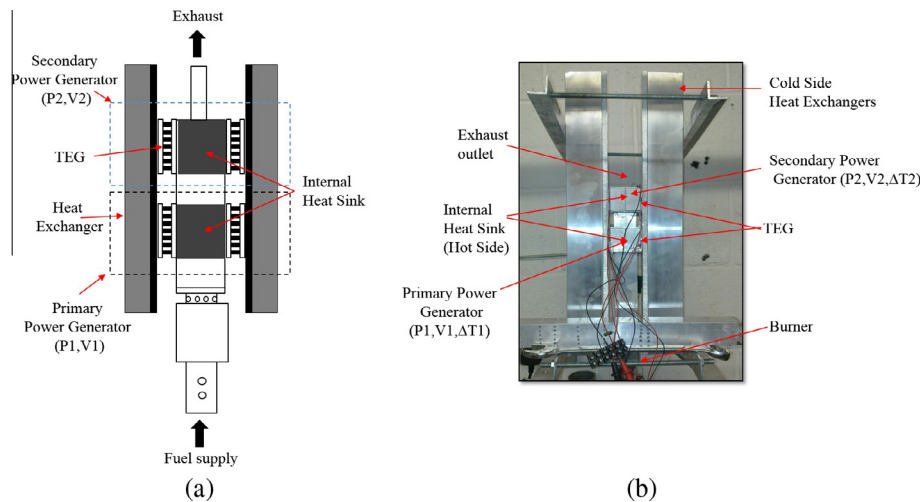


Fig. 6. (a) Schematic diagram and (b) photograph showing arrangement of TEGs, heat exchangers and power generators in configuration 1.

at a propane flowrate of 150 mL min^{-1} . Table 1 shows hot side temperatures (T_{H1} and T_{H2}) and temperature differences (ΔT_1 and ΔT_2) obtained from the two power generators. Results showed that the hot side temperature (T_{H2}) of the secondary power generator

was significantly less than that of the primary power generator (T_{H1}). Similar results for temperature difference were shown by the two power generators with primary (ΔT_1) having more than double the temperature difference achieved by secondary (ΔT_2).

Table 1
Hot side temperature (T_H) and temperature difference (ΔT) for configuration 1.

Hot side temperature of primary power generator, T_{H1} (K)	Hot side temperature of secondary power generator, T_{H2} (K)	Temperature difference of primary power generator, ΔT_1 (K)	Temperature difference of primary power generator, ΔT_2 (K)
427.1	347.4	71.4	31.4

Table 2
Power generation and load voltage output for configuration 1.

Load voltage: primary power generator, V_{L1} (V)	Load voltage: secondary power generator, V_{L2} (V)	Power output: primary power generator, P_1 (W)	Power output: secondary power generator, P_2 (W)	Total power output, P (W)
3.3	1.57	2.09	0.48	2.57

The electrical performance of the configuration 1 is shown in Table 2. The power generation and load voltage of primary power generator (P_1 and V_1) were higher than the secondary (P_2 and V_2). The power generation from the secondary power generator was 0.48 W, which was considerably less than the power generation of 2.09 W by the primary generator. The combined power generation was 2.57 W. It is evident from these results that having two power generators in series does not contribute towards improvement in electrical power output because the total amount of heat available is limited to 250 W. The secondary power generator does not receive enough heat to achieve a significant temperature difference, thus producing very little additional power. Hence, considering the cost of using two extra modules and limited amount of heat available, this configuration is not a practical solution at achieving higher performance from the system.

3.2.2. Configuration 2

This configuration, as similar to the previous one, consisted of four TEG modules, however in this case the placement of modules on the burner was different. The primary power generator did not consist of internal heat sink, which means that the two modules were placed directly on the sides of the burner exhaust tube. The secondary power generator consisted of an internal heat sink which accommodated the other two TEG modules. The idea was

Table 3
Hot side temperature (T_H) and temperature difference (ΔT) for configuration 2.

Hot side temperature of primary power generator, T_{H1} (K)	Hot side temperature of secondary power generator, T_{H2} (K)	Temperature difference of primary power generator, ΔT_1 (K)	Temperature difference of primary power generator, ΔT_2 (K)
385.5	414.7	51.5	65.6

to provide a separate heat exchanger for each TEG module, as shown in the schematic diagram in Fig. 7(a).

The design concept behind this configuration was to achieve higher temperature difference by providing a separate heat exchanger for each TEG module. Table 3 shows the hot side temperatures and temperature differences obtained with configuration 2, it can be seen that T_{H2} was higher than T_{H1} of configuration 1 involving two power generators. This is attributed to the presence of the IHS in the secondary power generator which was capturing more heat from the exhaust as compared to the primary power generator which does not have an IHS. Also, in contrast to configuration 1, this configuration has a higher T_{H2} than T_{H1} . The primary power generator, as mentioned earlier, is directly placed on the walls of the burner without having internal fins, and hence does not get hotter than 385 K, which is lower than T_{H1} of configuration 1. The temperature differences achieved by the two power generators are however in a similar range on the lower side as shown in Table 3.

Table 4 shows the load voltage output and corresponding power generation from configuration 2. Due to the lower temperature differences, the combined power generation was recorded to be comparatively low, 2.47 W. The reason behind this inferior electrical output can be attributed to the heat extraction pattern of the two power generators. The primary power generator, being closer to the flame, was achieving a T_{H1} of around 385 K without IHS which was lower than configuration 1 and hence ΔT_1 was low. Due to the presence of internal fins in the secondary power generator, it was able to achieve 414 K of T_{H2} which was higher than T_{H2} achieved by the secondary power generator of configuration 1.

3.2.3. Configuration 3

This design configuration consisted of 3 TEG modules, two used in a power generator and one placed on top of a chimney, as shown in Fig. 8(a). It can be seen that the chimney turns the flow through 90°, into the horizontal plane on leaving the burner exit. This

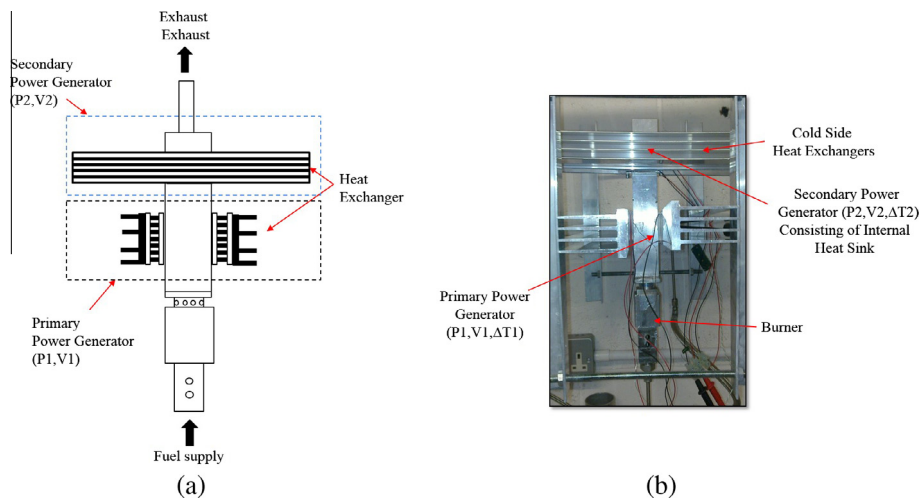


Fig. 7. (a) Schematic diagram and (b) photograph showing arrangement of TEGs, heat exchangers and power generator in configuration 2.

Table 4
Power generation and load voltage output for configuration 2.

Load voltage: primary power generator, V_{L1} (V)	Load voltage: secondary power generator, V_{L2} (V)	Power output: primary power generator, P_1 (W)	Power output: secondary power generator, P_2 (W)	Total power output, P (W)
2.3	2.75	1.02	1.45	2.47

configuration was aimed at increasing heat extraction from the exhaust gas. The chimney allowed the exhaust to impinge upon the top surface.

Fig. 8(b) shows a photograph of the configuration 3 being tested with 150 mL min^{-1} of propane supply to the burner, it can be seen that water vapour accumulated on the internal face of the chimney tube where the exhaust was made to change direction and leave horizontally. This was due to the fact that the exhaust had already been cooled below the H_2O dew point because of heat lost in the primary power generator and along the passage where it had to travel before reaching the top of the chimney. The water vapour was observed to interfere with the combustion during few test runs when it travelled upstream into the combustion chamber and causing the flame to extinguish.

Table 5 shows the temperature measurements from configuration 3; similar to configuration 1, the T_{H2} was significantly lower than T_{H1} and hence ΔT_2 being lower than ΔT_1 . The electrical performance of this configuration (shown in Table 6) was lower than the output of nominal configuration, while it was more than configuration 1 and 2. The individual performance of power generators was again similar to configuration 1; the primary power generator producing much higher power, 2.7 W, than 0.22 W produced by the secondary generator. The ΔT_2 achieved was low because of lower T_{H2} and hence lower P_2 which eventually caused the combined power output to be lower.

3.2.4. Summary

The comparison among the configurations showed that the power generation does not increase by increasing the number of TEG modules in the device. This can be showed by the comparison between configuration 1 and nominal configuration, the former generated 2.57 W of power using four TEG modules whereas the later generated 3.54 W using only two modules. The reason behind this can be attributed to the limited heat available to the modules, as the burner was allowed to combust only 150 mL min^{-1} of fuel in order to satisfy the operating requirements. When the number of

Table 5
Hot side temperature (T_H) and temperature difference (ΔT) for configuration 3.

Hot side temperature of primary power generator, T_{H1} (K)	Hot side temperature of secondary power generator, T_{H2} (K)	Temperature difference of primary power generator, ΔT_1 (K)	Temperature difference of primary power generator, ΔT_2 (K)
433.1	328.6	80	13.6

Table 6
Power generation and load voltage output for configuration 3.

Load voltage: primary power generator, V_{L1} (V)	Load voltage: secondary power generator, V_{L2} (V)	Power output: primary power generator, P_1 (W)	Power output: secondary power generator, P_2 (W)	Total power output, P (W)
3.75	0.77	2.7	0.23	2.93

modules were increased in a particular configuration, the amount of heat available to each module was low, which resulted in a lower temperature difference across it, and hence lower power output. The nominal configuration was proved to be the optimum design configuration because it uses the minimum number of TEG modules i.e. two and hence requires minimum number of heat exchangers and has shown to generate reasonable power.

3.3. Feasibility analysis: effect of ambient temperature

The nominal configuration was tested in an environment chamber where it was operated under different chamber temperatures. The aim of these experiments was to observe the effect of ambient temperature on power generation. Fig. 9 shows the setup of equipment inside the environment chamber which was isolated from the ambient.

Three values of chamber temperature were considered: 293, 303 and 313 K. The thermal power output of the burner was constant at 250 W, just as for the preceding tests. The device was operated for a minimum of 8 h continuously at a given chamber temperature.

The graph in Fig. 10(a) shows T_H at different ambient temperatures established inside the environmental chamber. It can be seen that there was around 5 K increase in the hot side temperature when the chamber temperature increased from 293 to 313 K. This increase in the hot side temperature is attributed to the fact that at higher chamber temperatures, the inlet air to the burner is warmer

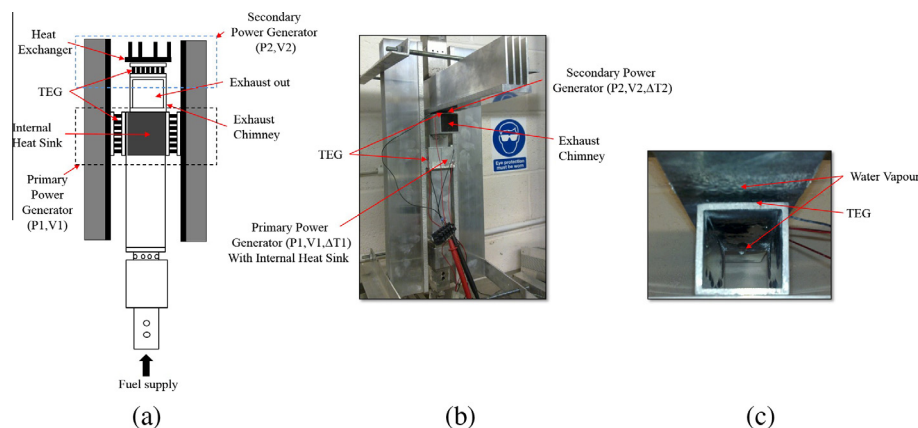


Fig. 8. (a) Schematic diagram, (b) photograph showing arrangement of TEGs, heat exchangers, and power generator in configuration 3, and (c) photograph showing water vapour accumulated in the exhaust chimney.

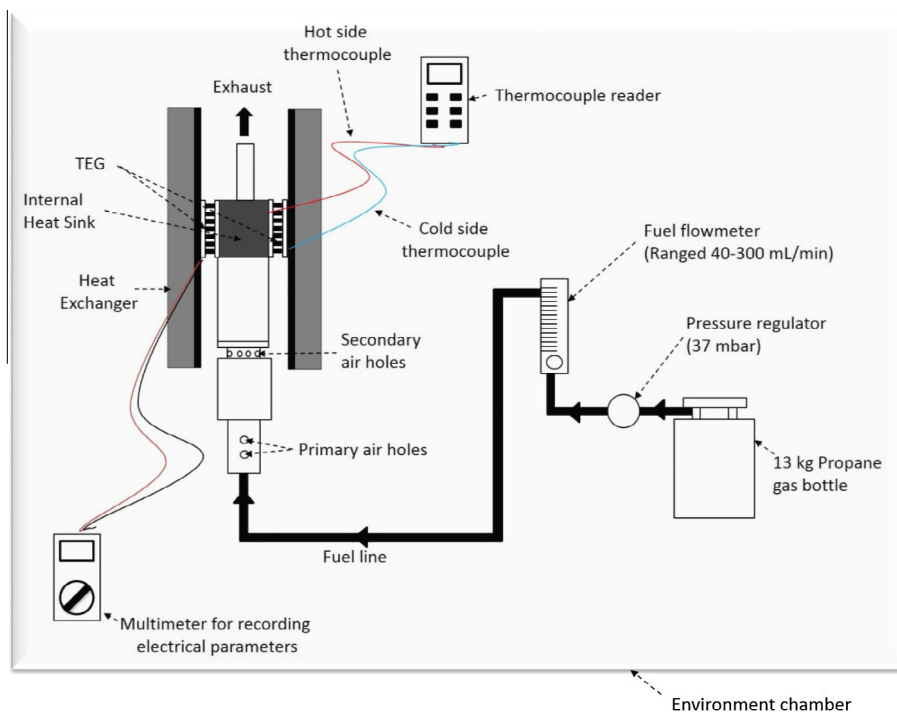


Fig. 9. Schematic of experimental setup of equipment.

causing the combustion temperature to increase. An approximately 13 K increase in the cold side temperature was observed when the chamber temperature was increased from 293 to 313 K, as shown in the graph in Fig. 10(b). This is an effect caused by low dissipation of heat by the heat exchangers at higher chamber temperatures. The increase in both cold and hot side temperature has an effect on the temperature difference and hence, output voltage and maximum power output of thermoelectric modules.

The graph in Fig. 10(c) shows temperature difference at different chamber temperatures. It is evident that the temperature difference decreased with increase in chamber temperature. This can be attributed to the higher cold side temperature causing the relative temperature difference magnitude to decrease.

The electrical parameters such as matched load voltage, power and current are shown in Fig. 10(d), (e) and (f), respectively. It can be seen that all the electrical parameters decrease with increase in chamber temperature. This can be attributed to the decrease in temperature difference at higher chamber temperatures. As mentioned previously, according to Seebeck principle, the power output is a function of temperature difference, and a decrease in temperature difference lowers the power output. This test proved the feasibility of generating electrical power using thermoelectric power generation principle even at conditions where ambient temperature is around 313 K.

3.4. Conclusion

The paper investigates design considerations and presents results from a meso-scale premixed non catalytic burner integrated with thermoelectric power generation modules. A 250 W premixed propane burner was developed having a backward facing step for enhancement of reactant mixing and secondary air addition into the combustion chamber as a means of flame stabilisation. The results showed that the combustion was complete with no measurable UHC present in the exhaust. The CO_2 production rate was found to be 450 mL min^{-1} , in line with predicted calculations based on combustion stoichiometry. The concentrations of

CO and NO_x were found to be 72 ppmV and 29 ppmV respectively, which were not considered significantly high for the application of the device.

Results from integration of burner with thermoelectric power generation modules showed that the hot side of the module can be optimised by employing internal heat sinks in the burner tube which helps in extracting more heat from the exhaust as the internal fins increase the surface area in contact with the exhaust gas. In this way, the amount of heat transferred to the TEG module can be increased, which ultimately increases the power output.

Investigation of four different design configurations showed that increasing the number of TEG modules in the system does not increase the power generation as the amount of heat available is limited to a 250 W burner output. A greater number of modules in the system meant less heat available to each module and hence lower power generation per module. Out of the four configurations tested, the nominal configuration, which consisted of two TEG modules, two heat exchangers and 1 IHS proved to be the most promising in terms of performance and potential cost.

The experimental investigation of the thermoelectric generator integrated with a meso-scale burner operating at different ambient temperatures has shown that the electrical power output decreases with an increase in the ambient temperature because of a decrease in the relative temperature difference. The major factor affecting the decrease in temperature difference was found to be increased cold side temperature at higher chamber or ambient temperatures. A reasonable electrical power, $\sim 3.5 \text{ W}$, was generated at the highest chamber temperature of 313 K. A stable premixed flame was observed throughout the operation of the burner at all the chamber temperatures. Therefore, it can be concluded that this study proves the operational feasibility of a meso-scale thermoelectrics and combustion system working together to generate enough electrical power to run small scale electronic devices while maintaining a clean and stable combustion for long durations of operation at elevated ambient temperatures.

This study was carried out with the aim of a device which can operate continuously for a month and the focus was given on a

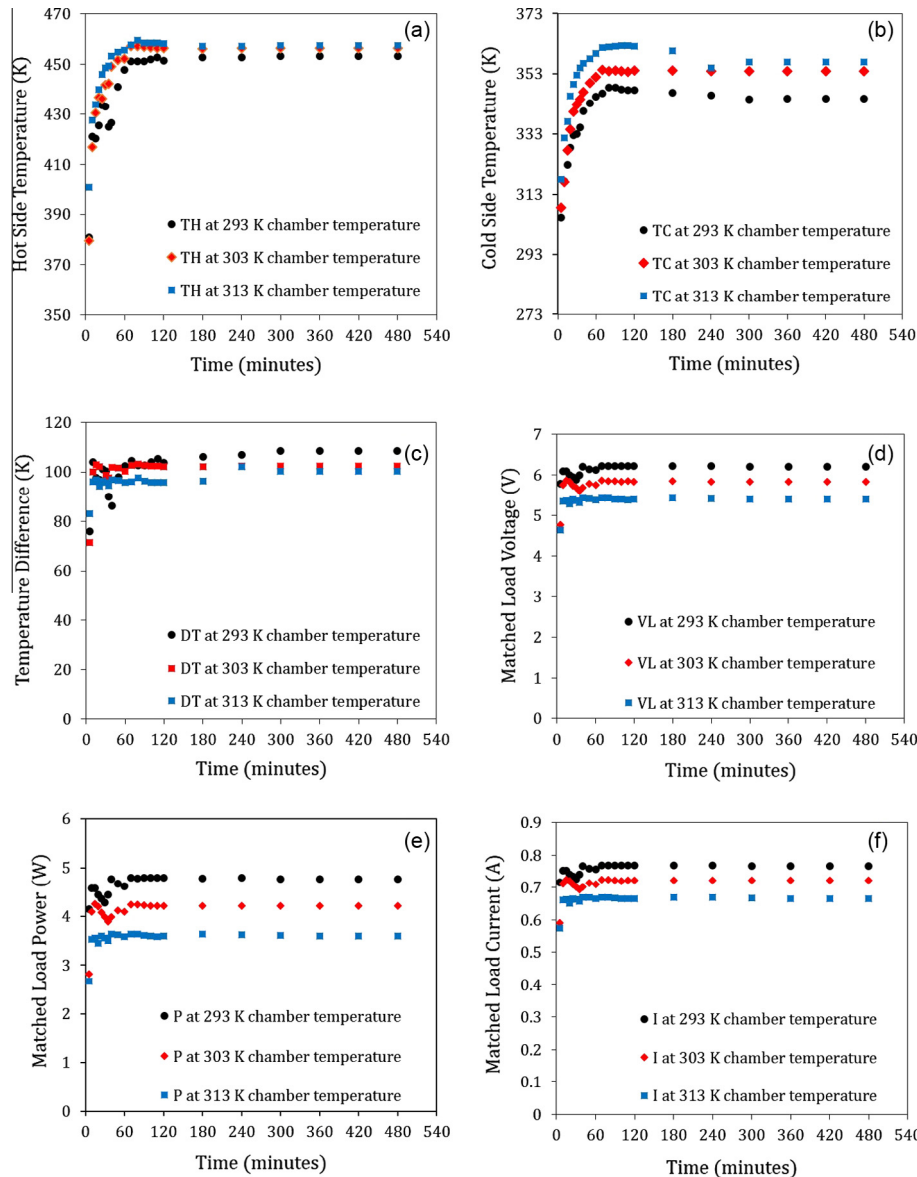


Fig. 10. Graphs showing (a) hot side temperature (T_H), (b) cold side temperature (T_C), (c) temperature difference, (d) matched load voltage, (e) matched load power output and (f) matched load current at different ambient temperature settings in the environmental chamber.

practical design solution which is low cost and does not require auxiliary components for its operation in remote areas. The future work can include varying the mass flow rate of the fuel and investigating its effect on thermoelectric performance.

Acknowledgements

The work was carried out under Knowledge Transfer Partnership (KTP partnership number 7509) and was financially supported by Technology Strategy Board (TSB) and the company partner, Agrisence BCS (now trading as Suterra). The authors gratefully acknowledge the support from Dr. Owen Jones, chairman of the KTP program.

References

[1] Federici JA, Norton DG, Bruggemann T, Voit KW, Wetzel ED, Vlachas DG. Catalytic microcombustors with integrated thermoelectric elements for portable power production. *J Power Sources* 2006;161:1469–78.

[2] Sonoc A, Jeswiet J, Soo Vi Kie. Opportunities to improve recycling of automotive lithium ion batteries. *Proc CIRP* 2015;29:752–7.

[3] Selvan KV, Ali MSM. Micro-scale energy harvesting devices: review of methodological performances in the last decade. *Renew Sustain Energy Rev* 2016;54:1035–47.

[4] Maruta K. Micro and mesoscale combustion. *Proc Combust Inst* 2011;33:125–50.

[5] Rowe DM. *CRC handbook of thermoelectrics*. Florida: CRC Press; 1995.

[6] Woodstream Corporation, Mosquito Magnet – How It Works, Available: <<http://www.mosquitomagnet.com/advice/how-it-works>> [last accessed: 11th January 2014].

[7] Yadav S, Yamasani P, Kumar S. Experimental studies on a micro power generator using thermo-electric modules mounted on a micro-combustor. *Energy Convers Manage* 2015;99:1–7.

[8] Norton DG, Voit KW, Bruggemann T, Vlachos DG. Portable power generation via integrated catalytic microcombustion-thermoelectric devices. Army Research Laboratory, Weapons and Materials Research Directorate.

[9] Xiao H, Qiu K, Gou X, Ou Q. A flameless catalytic combustion-based thermoelectric generator for powering electronic instruments on gas pipelines. *Appl Energy* 2013;112:1161–5.

[10] Merotto L, Fanciulli C, Dondè R, De Iulii S. Study of a thermoelectric generator based on a catalytic premixed meso-scale combustor. *Appl Energy* 2016;162:346–53.

[11] Merotto L, Dondè R, De Iulii S. Study of the performance of a catalytic premixed meso-scale burner. *Exp Thermal Fluid Sci* 2015;73:115–21.

- [12] Mustafa KF, Abdullah S, Abdullah MZ, Sopian K, Ismail AK. Experimental investigation of the performance of a liquid fuel-fired porous burner operating on kerosene-vegetable cooking oil (VCO) blends for micro-cogeneration of thermoelectric power. *Renew Energy* 2015;74:505–16.
- [13] Mustafa KF, Abdullah S, Abdullah MZ, Sopian K. Combustion characteristics of butane porous burner for thermoelectric power generation. *J Combust* 2015;2015. Article ID 121487, 13 pages. <http://dx.doi.org/10.1155/2015/121487>.
- [14] Mueller KT, Waters O, Bubnovich V, Orlovskaya N, Chen R. Super-adiabatic combustion in Al_2O_3 and SiC coated porous media for thermoelectric power conversion. *Energy* 2013;56:108–16.
- [15] Aranguren P, Astrain D, Rodríguez A, Martínez A. Experimental investigation of the applicability of a thermoelectric generator to recover waste heat from a combustion chamber. *Appl Energy* 2015;152:121–30.
- [16] Zhang Y, Wang X, Cleary M, Schoensee L, Kempf N, Richardson J. High-performance nanostructured thermoelectric generators for micro combined heat and power systems. *Appl Therm Eng* 2015;96:83–7.
- [17] Zhao M, Zhang H, Hua Z, Zhang Z, Zhang J. Performance characteristics of a direct carbon fuel cell/thermoelectric generator hybrid system. *Energy Convers Manage* 2015;89:683–9.
- [18] Hasani M, Rahbar N. Application of thermoelectric cooler as a power generator in waste heat recovery from a PEM fuel cell – an experimental study. *Int J Hydrogen Energy* 2015;40:15040–51.
- [19] Montecucco A, Siviter J, Knox AR. Combined heat and power system for stoves with thermoelectric generators. *Appl Energy* 2015. <http://dx.doi.org/10.1016/j.apenergy.2015.10.132> [in press].
- [20] O'Shaughnessy SM, Deasy MJ, Doyle JV, Robinson AJ. Adaptive design of a prototype electricity-producing biomass cooking stove. *Energy Sustain Dev* 2015;28:41–51.
- [21] Kariuki J, Balachandran R. Experimental investigation of dynamics of premixed acetylene-air flames in a micro-combustor. *Exp Thermal Fluid Sci* 2010;34:330–7.
- [22] Kania T, Dreizler A. Investigation of micro combustion chamber for a thermoelectric energy converter. In: *Proceedings of the European combustion meeting* (2009).
- [23] US Government. Micro combustor and combustion based thermoelectric micro generator-US Patent 6613972 B2; 2000.
- [24] Wu M, Wang Y, Yang V, Yetter RA. Combustion in meso-scale vortex chambers. *Proc Combust Inst* 2007;31:3235–42.
- [25] Belmont EL, Schoegl I, Ellzey JL. Experimental and analytical investigation of lean premixed methane/air combustion in a mesoscale counter-flow reactor. *Proc Combust Inst* 2013;34:3361–7.
- [26] Li J, Chou SK, Huang G, Yang WM, Li ZW. Study on premixed combustion in cylindrical micro combustors: transient flame behaviour and wall heat flux. *Exp Thermal Fluid Sci* 2009;33:764–73.
- [27] Li ZW, Chou SK, Shu C, Yang WM. Effects of step height on wall temperature of a microcombustor. *Inst Phys Publ* 2005;15:207–12.
- [28] Hong X, Wenming Y, Chou SK, Chang S, Zhigwang L. Microthermophotovoltaics power system for portable MEMS devices. *Microscale Thermophys Eng* 2005;9:85–97.
- [29] Yang WM, Chou SK, Shu C, Li ZW, Xue H. Combustion in micro-cylindrical combustors with and without a backward facing step. *Appl Therm Eng* 2002;22:1777–87.
- [30] Rowe DM, Bhandari CM. *Modern thermoelectrics*. London: Rinehart and Winston; 1983.
- [31] Rowe DM. *CRC handbook of thermoelectrics: micro to nano*. London: CRC Press; 2005.
- [32] Rowe DM, Min G. Conversion efficiency of thermoelectric combustion systems. *Trans Energy Convers* 2006;22.
- [33] Rowe DM, Min G. A novel principle allowing rapid and accurate measurement of a dimensionless thermoelectric figure of merit. *Meas Sci Technol* 2001;12:1261–2.
- [34] Rowe DM, Min G, Kontostavlakis K. Thermoelectric figure of merit under large temperature difference. *J Phys D: Appl Sci* 2004;37:1301–4.
- [35] Lesagea FJ, Pelletiera R, Fourniera L, Sempelsc EV. Optimal electrical load for peak power of a thermoelectric module with a solar electric application. *Energy Convers Manage* 2013;74:51–9.